Robust bursting to the origin; heteroclinic cycles with maximal symmetry equilibria

David Hawker and Peter Ashwin
Department of Mathematical Sciences,
Laver Building,
University of Exeter,
Exeter EX4 4QE, UK

September 22, 2004

Abstract

Robust attracting heteroclinic cycles have been found in many models of dynamics with symmetries. In all previous examples, robust heteroclinic cycles appear between a number of symmetry broken equilibria. In this paper we examine the first example where there are robust attracting heteroclinic cycles that include the origin, ie a point with maximal symmetry. The example we study is for vector fields on $\mathbb{R}^3$ with $(\mathbb{Z}_2)^3$ symmetry. We list all possible generic (codimension one) local and global bifurcations by which this cycle can appear as an attractor; these include a resonance bifurcation from a limit cycle, direct bifurcation from a stable origin and direct bifurcation from other and more familiar robust heteroclinic cycles.

AMS classification scheme numbers: 34C37, 37C80.

1 Introduction

Consider an ordinary differential equation (ODE) on $\mathbb{R}^n$ that is symmetric under the action of a finite group G acting on $\mathbb{R}^n$. In addition to symmetric versions of the usual attractors that arise in generic systems, symmetries can force the appearence of robust asymptotically stable heteroclinic cycles or networks between saddle equilibria. These attractors consist of a network of saddle equilibria connected via trajectories that are robust because they lie within invariant subspaces forced by the symmetries. We refer to [Guckenheimer & Holmes, 1988, Krupa, 1997, Ashwin & Field, 1999, Ashwin & Montaldi, 2002] for background and some examples, and [Krupa & Melbourne, 1995, Krupa & Melbourne, 2004] for characterization of examples of robust homoclinic cycles in low dimensions.

In Guckenheimer & Holmes [1988], Armbruster *et al.* [1988], Field & Swift [1991] and Melbourne *et al.* [1989], robust heteroclinic cycles arise at generic local bifurcation of the origin.

In such cases centre manifold and normal form reduction reduces to an ODE that is a low order polynomial equation on a subspace on which G acts irreducibly [Golubitsky *et al.*, 1988]. In such cases all eigenvalues of the linearization of origin on the center manifold are equal, the origin cannot be saddle and hence cannot be included in any robust heteroclinic cycle contained within the centre manifold.

However, robust heteroclinic cycles can be created by global bifurcations and in such cases there is no reason for them to be contained in any centre manifold; the origin may be an equilibrium on the cycle. This paper shows there are robust heteroclinic attractors to the origin for smooth ODEs on $\mathbb{R}^3$ with symmetry $G = (\mathbb{Z}_2)^3$. Note that these cycles do not fit into the class of 'simple' robust heteroclinic cycles studied by Krupa and Melbourne [1995,2004]; they do however form a subspace of those studied by Kirk & Silber [1994] who examined competing cycles on $\mathbb{R}^4$ with $(\mathbb{Z}_2)^4$ symmetry, though restricted to those with non-zero axes equilibria.

More precisely, consider smooth ODEs X_G on $\mathbb{R}^3$ that respect the group of symmetries $G = (\mathbb{Z}_2)^3$ generated by the reflections κ_i, $i = 1, 2, 3$ acting by

$$\begin{aligned}\kappa_1(x, y, z) &= (-x, y, z)\\ \kappa_2(x, y, z) &= (x, -y, z)\\ \kappa_3(x, y, z) &= (x, y, -z).\end{aligned}$$

Observe that the positive octant

$$\mathcal{O} = \{(x, y, z) \ : \ x \geq 0, \ y \geq 0, \ z \geq 0\}$$

is invariant and we restrict most of our computations to this; note that $G\mathcal{O} = \mathbb{R}^3$. For an equilibrium P we define the stable, unstable and center manifolds ($W^s(P)$, $W^u(P)$ and $W^c(P)$ respectively) as usual (see e.g. [Perko, 2001]). Our main result is the following:

Theorem 1 *There is a non-empty open set $U \subset X_G$ such that each $f \in U$ has a robust attracting heteroclinic cycle in $\mathcal{O}$ between the origin P_0 and equilibria P_1 and P_2 with one-dimensional connections:*

$$(W^u(P_k) \cap \mathcal{O}) \subset W^s(P_{k+1}) \tag{1}$$

for $k = 0, 1, 2$ modulo 3.

We postpone the proof of Theorem 1 to Section 2 as the proof involves several steps. These steps include considering an explicit example with a robust cycle; we show that this is attracting and that it is robust to an open set of perturbations in X_G. Our other result is a characterization of possible bifurcation of such cycles.

Theorem 2 *Consider U as in Theorem 1 and suppose that f_s is a smooth family in X_G ($s \in \mathbb{R}$) such that $f \in U$ for $s > 0$ and $f \notin U$ for $s < 0$. Then at least one of the cases listed in Table 1 occurs for f_0. Generically precisely one of these conditions occurs. Moreover, in the generic cases 1a-c then* $\dim(W^c(P_k)) = 1$.

Case	Event
$1a$	$\dim(W^c(P_0)) \geq 1$
$1b$	$\dim(W^c(P_1)) \geq 1$
$1c$	$\dim(W^c(P_2)) \geq 1$
$2a$	$W^u(P_0) \cap W^s(P_1) = \emptyset$
$2b$	$W^u(P_1) \cap W^s(P_2) = \emptyset$
$2c$	$W^u(P_2) \cap W^s(P_0) = \emptyset$.
3	The cycle satifies a resonance condition (see Lemma 3).

Table 1: The cases leading to loss of the robust attracting heteroclinic cycle in Theorem 2.

Section 3 analyses these generic bifurcations that create or destroy the robust attracting cycle. Among the possibilities listed in Theorem 2 we find a number of generic bifurcation scenarios giving for example:

1a Bifurcation to an attracting heteroclinic cycle topologically equivalent to that of Guckenheimer and Holmes [1988], or bifurcation to a stable origin.

2c Bifurcation to a non-robust heteroclinic cycle.

3 Bifurcation to an attracting limit cycle.

Section 4 finishes with a discussion of sufficient and necessary conditions for the appearence of similar robust cycles to the origin. We also discuss how such cycles should manifest themselves in the dynamics of physical systems.

2 Robustness of heteroclinic attractors to the origin

Any vector field in X_G with this symmetry will leave the subspaces

$$\Sigma_k = \text{fix}(\langle \kappa_k \rangle) = \{(x_1, x_2, x_3) \ : \ x_k = 0\}$$

invariant, for $k = 1, 2, 3$. Moreover, one can write any $f \in X_G$ as

$$\begin{array}{rcl} \dot{x} & = & x f_1(x^2, y^2, z^2) \\ \dot{y} & = & y f_2(x^2, y^2, z^2) \\ \dot{z} & = & z f_3(x^2, y^2, z^2) \end{array} \tag{2}$$

for $f_i \in C^\infty(\mathbb{R}^3, \mathbb{R})$. A particular case is the fifth order polynomial ODE

$$\begin{array}{rcl} \dot{x} & = & x(\alpha_0 + \alpha_1 x^2 + \alpha_2 y^2 + \alpha_3 z^2 \\ & & +\alpha_{12} x^2 y^2 + \alpha_{13} x^2 z^2 + \alpha_{23} y^2 z^2 + \alpha_{11} x^4 + \alpha_{22} y^4 + \alpha_{33} z^4) \\ \dot{y} & = & y(\beta_0 + \beta_1 x^2 + \beta_2 y^2 + \beta_3 z^2 \\ & & +\beta_{12} x^2 y^2 + \beta_{13} x^2 z^2 + \beta_{23} y^2 z^2 + \beta_{11} x^4 + \beta_{22} y^4 + \beta_{33} z^4) \\ \dot{z} & = & z(\gamma_0 + \gamma_1 x^2 + \gamma_2 y^2 + \gamma_3 z^2 \\ & & +\gamma_{12} x^2 y^2 + \gamma_{13} x^2 z^2 + \gamma_{23} y^2 z^2 + \gamma_{11} x^4 + \gamma_{22} y^4 + \gamma_{33} z^4) \end{array} \tag{3}$$

Fixed point	x	y	z
P_0	$e_0 = 4$	$-c_0 = -4$	$-d_0 = -1$
P_1	$-d_1 = -8$	$e_1 = 4$	$-c_1 = -3$
P_2	$-c_2 = -8$	$-d_2 = -24$	$e_2 = 3$

Table 2: Notation used for the eigenvalues of the model system (3) and their values for the parameter values in (4); these correspond to eigenvectors with a non-zero component in the direction given.

where α_i, β_i and γ_i are fixed parameters. We consider the dynamics of model (3) with parameters

$$\begin{gathered} \alpha_0 = 4,\ \alpha_1 = -1,\ \alpha_2 = -3, \\ \beta_0 = -4,\ \beta_1 = 2,\ \beta_2 = 5,\ \beta_3 = 1,\ \beta_{13} = -2,\ \beta_{22} = -1,\ \beta_{33} = -9, \\ \gamma_0 = -1,\ \gamma_1 = -0.5,\ \gamma_2 = 1,\ \gamma_3 = -0.01,\ \gamma_{23} = -0.2,\ \gamma_{33} = -0.01. \end{gathered} \tag{4}$$

and all others set to zero. Figure 1 shows the cycle computed numerically, whereas Figure 2 shows the cycle schematically related to the locations of the P_i and Q_i at these parameter values and introduces some notation used later on.

Theorem 3 *The system (3,4) has a heteroclinic cycle $P_0 \to P_1 \to P_2 \to P_0$ in $\mathcal{O}$ with P_0 the origin. This cycle is an asymptotically stable attractor within $\mathcal{O}$.*

Proof One can compute that the only equilibria in $\mathcal{O}$ are

$$\begin{gathered} P_0 = (0,0,0),\ P_1 = (2,0,0),\ P_2 = (0,2,0), \\ Q_0 = (0,1,0),\ Q_1 = (0,1.01997,0.428283), \\ R_0 = (0.525517,1.11413,0.627359) \end{gathered}$$

(to 6 significant figures). There are other equilibria in $\mathbb{R}^3$ on group orbit of these equilibria under the action of G and this gives a total of 19 equilibria for this system. One can verify by direct computation that all of the equilibria labelled P_i have eigenvalues as listed in Table 2; they clearly each have a two dimensional stable manifold and a one dimensional unstable manifold. We can compute that $(W^u(P_0) \cap \mathcal{O}) \subset W^s(P_1)$ because the system on $y = z = 0$ reduces to

$$\dot{x} = x(4 - x^2)$$

and this is positive for all $0 < x < 2$ giving the connecting orbit. We give proof that there are the other connections (1) in the Lemmas 1 and 2. We show that the cycle is an attractor in Lemma 3. **QED**

Lemma 1 *For the system (3,4) there is a connection $(W^u(P_1) \cap \mathcal{O}) \subset W^s(P_2)$.*

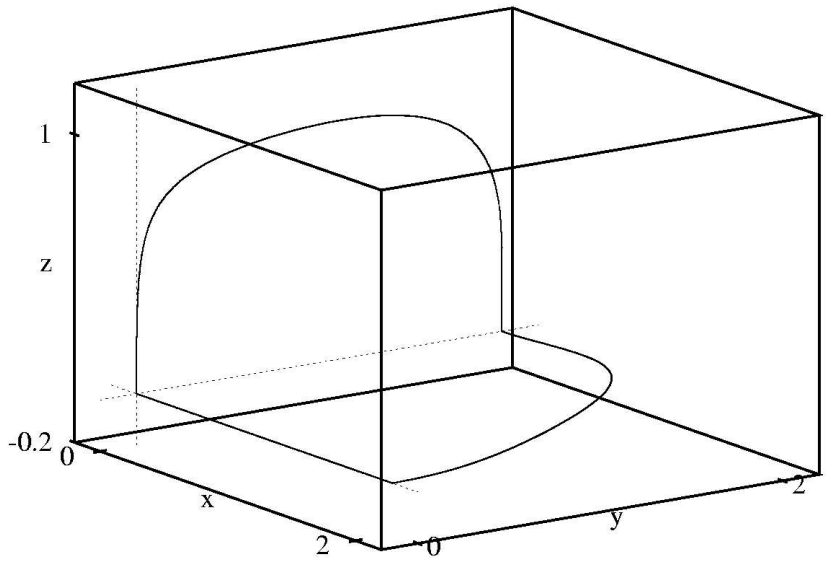

(a)

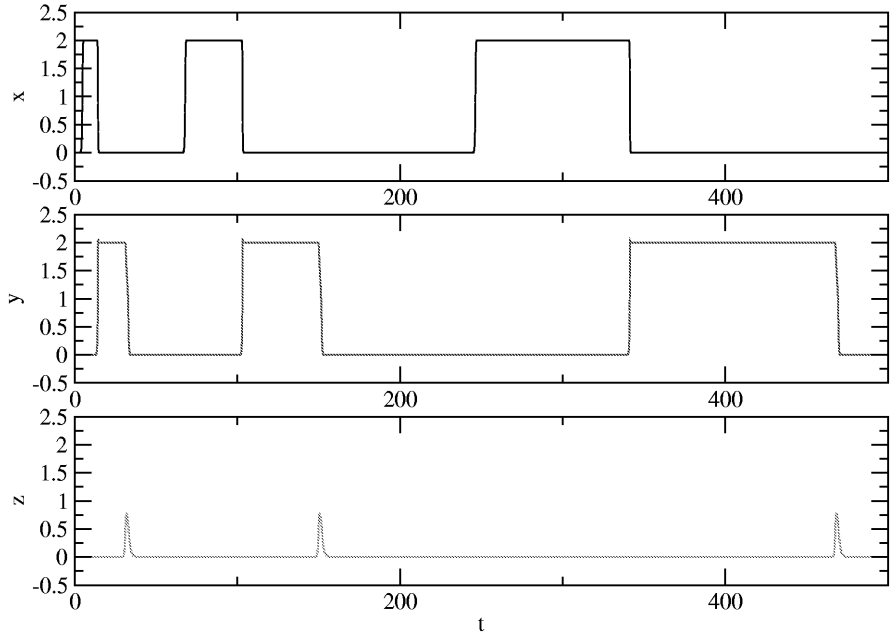

(b)

Figure 1: The attracting robust heteroclinic cycle for the ODE (3) at parameter values (4). (a) shows the cycle in (x, y, z) space while (b) shows the timeseries of a trajectory attracted to the cycle; observe that the origin forms part of the cycle. There are 8 possible cycles related by the symmetry group $G = (\mathbb{Z}_2)^3$.

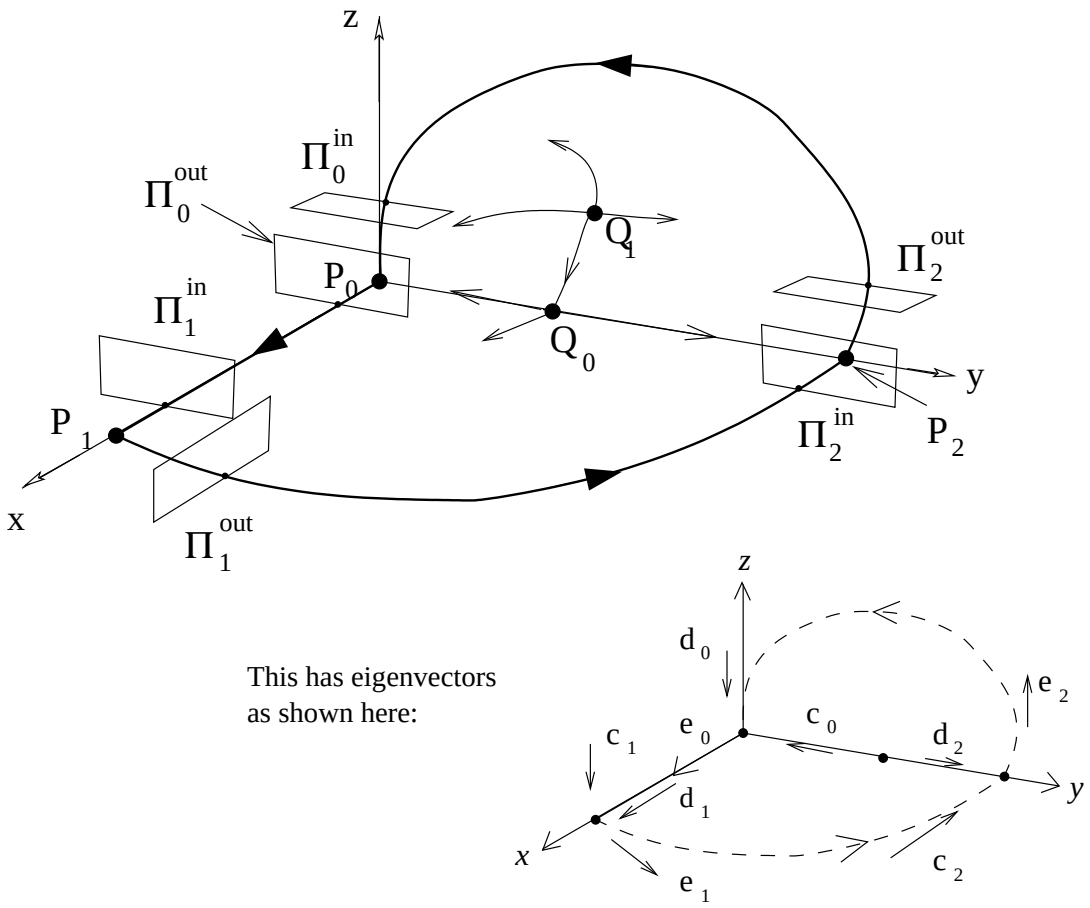

Figure 2: Schematic diagram showing the structure of the attracting robust heteroclinic cycle illustrated in Figure 1. The surfaces of section and the equilibria are labelled as in the text and the eigenvalues are labelled as in Table 2. The directions of the eigenvectors are as they would be locally for the cycle in Figure 1; the following section examines possible bifurcations when some of these directions are reversed, i.e. the eigenvalue passes through zero.

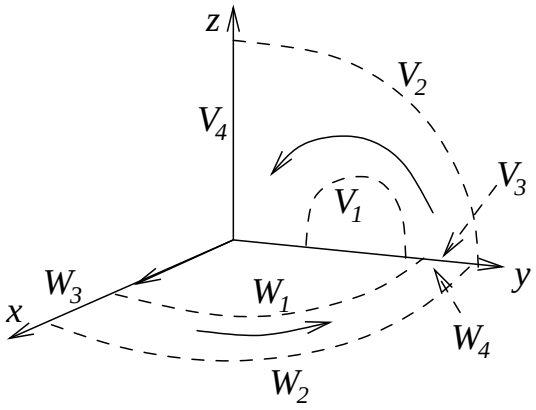

Figure 3: Schematic diagram showing the boundaries W_i of $\mathcal{W}$ and V_i of $\mathcal{V}$ used in the proof of Lemma 1 and 2 . The robust cycle is contained in the union of $\mathcal{W}$, $\mathcal{V}$ and the x-axis.

Proof Since the unstable direction for P_1 is within the plane $z = 0$ we reduce to

$$\begin{aligned}\dot{x} &= x(4 - x^2 - 3y^2)\\ \dot{y} &= y(-4 + 2x^2 + 5y^2 - y^4).\end{aligned}$$

Consider

$$L(x, y) = \frac{x^2}{x^2 + y^2}$$

and note that $L(x, 0) = 1$, $L(0, y) = 0$ and $L(x, y) > 0$ in the interior of $\mathcal{O}$. We claim that $\dot{L} < 0$ in some absorbing set $\mathcal{W}$ that connects P_1 and P_2 consisting of the compact region bounded by $\partial\mathcal{W} = W_1 \cap W_2 \cap W_3 \cap W_4$ where

$$W_k = \{(x, y, 0) \in \mathcal{O} \ : \ 2 - \epsilon_k = r = \sqrt{x^2 + y^2}\} \ \text{ for } \quad k = 1, 2$$

and W_3 and W_4 are segments for the x- and y-axes respectively. We choose ϵ_k so that $\dot{r} > 0$ on W_1, $\dot{r} < 0$ on W_2, $\dot{L} < 0$ in $\mathcal{W}$ and P_1 and P_2 are contained in $\mathcal{W}$. Note that W_3 and W_4 are subsets of invariant lines. Computing

$$\dot{r} = \frac{x^2}{\sqrt{x^2 + y^2}}(4 - x^2 - 3y^2) + \frac{y^2}{\sqrt{x^2 + y^2}}(-4 + 2x^2 + 5y^2 - y^4).$$

For a point $(x, y) \in W_k$ this gives

$$\begin{aligned}\dot{r} = \ & \tfrac{x^2}{2-\epsilon_k}\ (4 - x^2 - 3(2 - \epsilon_k)^2 + 3x^2) + \\ & \tfrac{(2-\epsilon_k)^2 - x^2}{2-\epsilon_k}(-4 + 2x^2 + 5(2 - \epsilon_k)^2 - 5x^2 - ((2 - \epsilon_k)^2 - x^2)^2)\end{aligned}$$

Concerning the Lyapunov function L one can compute that

$$\dot{L} = \frac{2xy^2}{(x^2 + y^2)^2}\ \dot{x} - \frac{2yx^2}{(x^2 + y^2)^2}\ \dot{y} = \frac{2x^2y^2}{(x^2 + y^2)^2}\ (8 - 3x^2 - 8y^2 + y^4).$$

By examining the maximum and minimum of $\dot{r}$ and $\dot{L}$ on $\mathcal{W} \subset \mathcal{O}$ using Maple, we can determine that (to 3 significant figures)

- If $0.0689 < \epsilon_1 < 1$ then $\dot{r} > 0$ on W_1
- If $0.452 < \epsilon_2$ then $\dot{r} < 0$ on W_2.
- If $0 < \epsilon_1 < 0.122$ and $0 < \epsilon_2 < 0.613$ then $\dot{L} > 0$ in $\mathcal{W} \setminus \{W_3, W_4\}$.

Hence if we choose for example $\epsilon_1 = 0.1$ and $\epsilon_2 = 0.5$ in the interior of these regions, we have established there is an absorbing region $\mathcal{W}$, that contains P_0 and P_1 but no other fixed points, for which all interior points limit to the y-axis, and in particular $(W^u(P_1) \cap \mathcal{O}) \subset W^s(P_2)$. **QED**

Lemma 2 *For the system (3,4) there is a connection* $(W^u(P_2) \cap \mathcal{O}) \subset W^s(P_0)$.

Proof Choose $M(y,z) = arctan(\frac{z^2}{y^2-1})$ with $0 \leq M \leq \pi$ and we will show that there is an absorbing region $\mathcal{V}$ on which $\dot{M} > 0$, similar to the proof of Lemma 1. We define $\mathcal{V}$ consisting of the compact region bounded by $\partial\mathcal{V} = V_1 \cap V_2 \cap V_3 \cap V_4$ where

$$V_1 = \{(0,y,z) \in \mathcal{O} \ : \ \epsilon_1 = z^4 + (y-1)^2 - 0.4y - 1\},$$
$$V_2 = \{(0,y,z) \in \mathcal{O} \ : \ \epsilon_2 = z^4 + (y-1)^2 - 1.5y - 1\},$$

and V_3 and V_4 are segments in the y and z axes respectively. We claim there is an ϵ_1 and ϵ_2 such that $\dot{M} > 0$ in $\mathcal{V}$ and $\mathcal{V}$ is absorbing. To see this, we compute that

$$\dot{M} = \frac{z^2}{y^4 - 2y^2 + 1 + z^4}(4y^2 - 8y^4 - 1.62y^2z^2 + 2y^6 + 17.98y^2z^4 - 0.4y^4z^2 + 2 + z^2 + z^4)$$

and by examining maxima and minima of the appropriate functions using Maple, we see that:

- If $-1.35 \leq \epsilon_1 \leq -0.79$ then all trajectories through V_1 enter $\mathcal{V}$.
- If $\epsilon_2 \geq 3.02$ then all trajectories through V_2 enter $\mathcal{V}$.
- If $-1.02 < \epsilon_1$ then $\dot{M} > 0$ on $\mathcal{V} \setminus \{V_3, V_4\}$.

Hence if we choose, for example, $\epsilon_1 = -1$ and $\epsilon_2 = 3.5$ then the equilibrium Q_1 is not in $\mathcal{V}$. This means that all trajectories in the interior of $\mathcal{V}$ limit to V_4 and hence to P_0; in particular $(W^u(P_2) \cap \mathcal{O}) \subset W^s(P_0)$. **QED**

2.1 Stability of the robust cycle to the origin

It remains to show that the robust heteroclinic cycle is an attractor. Referring to Figure 2 and Table 2, we approximate the return map local to the cycle by examining the flow near the hyperbolic equilibria; as is typical the attractiveness or otherwise of the cycle is determined purely by the a quantity derivable from the eigenvalues of the linearizations at the equilibria. For a cycle of the form (1) we define

$$\lambda = \frac{c_2(d_0e_1 + c_0c_1)}{e_0e_1e_2} \tag{5}$$

where the eigenvalues of the equilibria are labelled as in Table 2.

Lemma 3 *The cycle (1) is attracting if* $\lambda > 1$ *and repelling if* $\lambda < 1$.

Proof We place surfaces of section Π_i^{in} and Π_i^{out} at a distance ϵ from each P_i and take linearising coordinates near each of the P_i. Figure 2 shows the cycle with the equilibria P_i and their eigendirections labelled as in the Table. The first return map F to the section Π_0^{in} is given by

$$F = G_2 \circ F_2 \circ G_1 \circ F_1 \circ G_0 \circ F_0 \text{ where } F : \Pi_0^{\text{in}} \to \Pi_0^{\text{in}}.$$

where as before we consider only trajectories in $\mathcal{O}$ and the maps

$$\Pi_i^{\text{in}} \stackrel{F_i}{\to} \Pi_i^{\text{out}} \stackrel{G_i}{\to} \Pi_{i+1}^{\text{in}}.$$

for i modulo 3. Leading order terms for these maps are given in Appendix A giving the return map $F(x, y) = (x', y')$ where

$$\begin{aligned} x' = {} & Ax^{\frac{c_2(d_0e_1+c_1c_0)}{e_0e_1e_2}} y^{\frac{c_2c_1}{e_2e_1}}, \\ y' = {} & B + Cx^{\frac{d_2(d_0e_1+c_1c_0)}{e_2e_1e_0}} y^{\frac{c_1d_2}{e_1e_2}} + \\ & Dx^{\frac{d_2(d_0e_1+c_1c_0)+e_2d_1c_0}{e_2e_1e_0}} y^{\frac{c_1d_2+d_1e_2}{e_1e_2}} + \\ & Ex^{\frac{(d_2+e_2)(d_0e_1+c_1c_0)}{e_2e_1e_0}} y^{\frac{c_1(d_2+e_2)}{e_1e_2}}. \end{aligned} \tag{6}$$

For one dimensional unstable manifolds, generically the c_i, d_i and e_i are all positive and the A, B, C, D, E are non-zero. Near $x = 0$ the dominant terms are

$$\begin{aligned} x' = {} & Ax^{\frac{c_2(d_0e_1+c_1c_0)}{e_0e_1e_2}} y^{\frac{c_2c_1}{e_2e_1}}, \\ y' = {} & B \end{aligned} \tag{7}$$

for A and B positive constants. The cycle is stable precisely when $x \to 0$ and this is requires $\lambda > 1$ where λ is as in (5). Similarly, if $\lambda < 1$ then typical initial conditions near $x = 0$ will iterate away from it implying instability. **QED**

When $\lambda = 1$ the stability is determined by higher order terms and we say the cycle has a *resonance*; typically this gives rise to bifurcation of a periodic orbit from the cycle (see for

example [Chow *et al.*, 1990]). One can verify from Table 2 for the system (3,4) as illustrated in Figure 1 that $\lambda = \frac{8}{3}$, and so the cycle is an attractor in this case.

Note also that for the model (3) one can write λ in terms of the system parameters, assuming that the P_i exist and are as example above. In this case we have

$$\lambda = \frac{-(\alpha_0 + y_e^2\alpha_2)(x_e^2)(-\gamma_0\beta_1 + \beta_0\gamma_1)}{(\alpha_0)(\beta_0 + x_e^2\beta_1)(\gamma_0 + y_e^2\gamma_2)} \tag{8}$$

where y_e is the most positive solution of $\beta_0 + \beta_2 y_e^2 + \beta_{22} y_e^4 = 0$ and x_e is the most positive solution of $\alpha_0 + \alpha_1 x_e^2 + \alpha_{11} x_e^4 = 0$. We now gather together the results giving the proof of the main theorem:

Proof of Theorem 1 Consider the set $U_1 \subset X_G$ of f such that

(i) There is a hyperbolic equilibrium $P_1 = (x_0, 0, 0)$, $x_0 > 0$, with a one-dimensional unstable manifold in the direction $(0, \pm 1, 0)$.

(ii) There is a hyperbolic equilibrium $P_2 = (0, x_1, 0)$, $x_1 > 0$, with a one-dimensional unstable manifold in the direction $(0, 0, \pm 1)$.

(iii) $P_0 = (0, 0, 0)$ is hyperbolic with a one-dimensional unstable manifold in the direction $(\pm 1, 0, 0)$. We denote the eigenvalues of P_k as in Figure 2 and Table 2.

Within U_1 there is an open set U_2 such that for the flow within $\mathcal{O}$

$$W^u(P_0) \subset W^s(P_1), \quad W^u(P_1) \subset W^s(P_2) \quad \text{and} \quad W^u(P_2) \subset W^s(P_0),$$

and all these connections are transverse [Field, 1996] within some invariant subspace. Each of these connections is from a hyperbolic saddle with one dimensional unstable manifold and each connection is from saddle to sink within an invariant subspace and so the connections are robust to any smooth perturbations of the vector field that preserve the invariant subspaces. Within U_2 there is an open set U_3 on which the quantity $\lambda > 1$ and hence the cycle will be an (asymptotically stable) attractor. Finally, Theorem 3 demonstrates explicitly using the system (3,4) that U_3 is non-empty. **QED**

In the light of the proof above, the proof of Theorem 2 is relatively clear:

Proof of Theorem 2 Referring to the proof of Theorem 1 we note that if $f_\gamma \in U_2 \setminus U_3$ then we have case 3, if $f_\gamma \in U_1 \setminus U_2$ then we have case 2 and if $f_\gamma \notin U_1$ then at least one of the equilibria must be at a bifurcation point (case 1). **QED**

3 Generic bifurcations of the robust cycle to the origin

In this section we consider the generic codimension one bifurcations from U as in Theorem 2 in more detail and how the cause creation/destruction of the robust heteroclinic cycle to the origin. As in the statement of the Theorem, there are three main cases:

- Case 1a,1b,1c: Local bifurcations of one of the equilibria P_i.
- Case 2a,2b,2c: Global bifurcations that create or destroy connections.
- Case 3: Global resonance bifurcation of the cycle.

We consider each of these cases in turn, with some numerical examples from the explicit model system (3).

3.1 Case 1a: Local bifurcation at P_0

There are three generic bifurcations of the saddle P_0 associated with a change of sign of the eigenvalues in each of the directions x, y, z; these are all pitchfork bifurcations and we treat each of these in turn.

3.1.1 Bifurcation of P_0 in x-direction: stabilization of origin

On changing the sign of α_0 (the positive eigenvalue) one can cause the origin P_0 to undergo a bifurcation in the x direction. Only if this bifurcation is subcritical can we have a transition from a stable origin for $\alpha_0 < 0$ to an attracting heteroclinic cycle including the origin for $\alpha_0 > 0$. For $e_0 = \alpha_0 \to 0$ note that by (5) we have $\lambda \to \infty$, implying that the cycle will be stable after bifurcation and moreover it will be very strongly attracting in that only a few circuits of the cycle are likely to be seen numerically for small positive α_0.

In order to obtain such a subcritical bifurcation while still retaining an equilibria at P_1 we require additionally that $\alpha_{11} < 0$, and hence that $\alpha_1 > 0$. As an example, consider (3,4), except for $\alpha_1 = 1$ and $\alpha_{11} = -0.25$; we can then obtain such a bifurcation as α_0 passes through zero.

3.1.2 Bifurcation of P_0 in y-direction: creation of robust cycle to equilibria on y-axis

If P_0 loses stability supercritically in the y direction to a new equilibrium P_0' on the y axis, then this gives rise to a robust heteroclinic cycle involving P_0' and P_2 only. This bifurcation can occur as β_0 passes through zero.

Note that we need to introduce an extra seventh order coefficient β_{222} of y^7 in $\dot{y}$ as we require seven equilibria simultaneously on the y-axis for this generic scenario (see Figure 5). Hence we choose the parameters as in (3,4) except for

$$\begin{gathered}\alpha_0 = 2,\ \beta_0 = 0.01,\ \beta_2 = -2.1,\ \beta_{22} = 5,\ \beta_{222} = -2,\\ \gamma_0 = -2.5,\ \gamma_2 = \gamma_{23} = 3.\end{gathered} \tag{9}$$

Figure 4 illustrated this cycle between the two equilibria P_0', P_1. This cycle is topologically equivalent to the robust cycle observed in 1:2 resonance for bifurcations with symmetry $\mathbf{O}(2)$; see for example Krupa [1997], or for an example in a partial differential equation [Kevrekidis *et al.*, 1990].

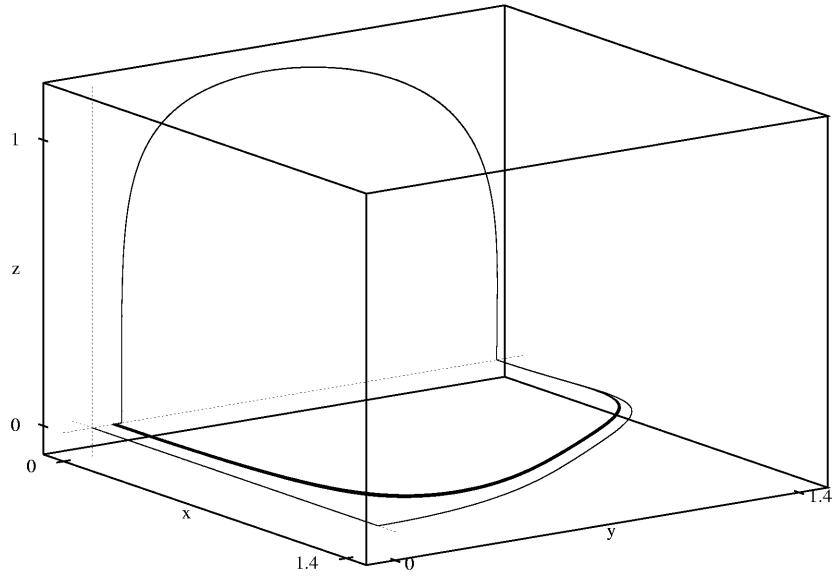

Figure 4: This shows a trajectory converging to a robust heteroclinic cycle between two equilibria in the y axis, not including the origin in the system (3). This cycle appears at a supercritical pitchfork bifurcation at the origin from the cycle shown in Figure 1.

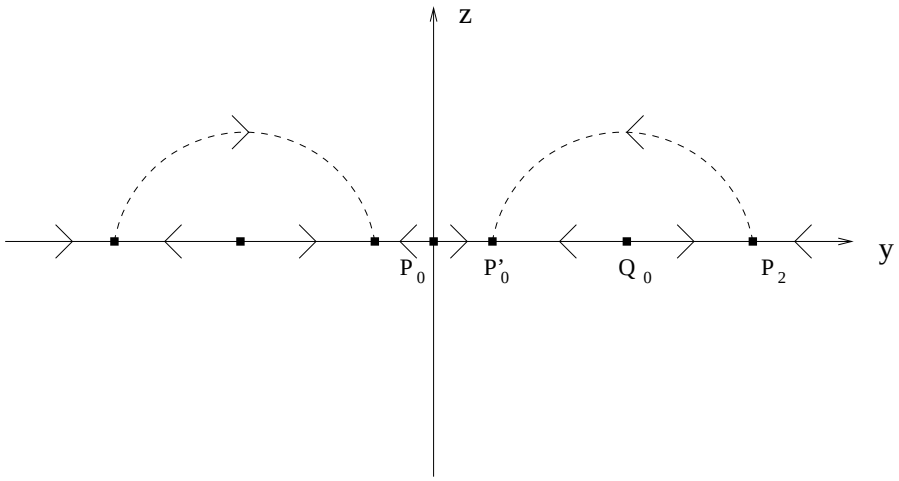

Figure 5: Schematic illustration of the equilibria needed for the existence of the robust cycle between P_0' and P_2 as seen in Figure 4.

3.1.3 Bifurcation of P_0 in z-direction; creation of Guckenheimer-Holmes cycle

The final bifurcation at P_0 that we consider occurs when it loses stability in the z direction, i.e. when γ_0 passes through zero. Only if this bifurcation is supercritical then we can bifurcate directly from a cycle equivalent to that in Figure 1 to a robust attracting cycle of the type observed by Guckenheimer and Holmes [1988]. Varying only γ_0, we can obtain such a bifurcation, however for (4) we also have a resonance bifurcation at the same point (see section 3.5); By setting for example $\gamma_1 = -0.6$ we can avoid this degeneracy.

Setting $\gamma_0 = 0.01$ there is a heteroclinic cycle as shown in Figure 6(a), which now also has equilibria at $(0, 0,\ 0.3)$. It is interesting to note that at the bifurcation point, $\gamma_0 = 0$, there is still a heteroclinic cycle even though one of the equilibria is now non-hyperbolic. We show the time series converging to this cycle in Figure 6(b), and one can observe that on approach to the origin, the rate of approach is slow, consistent with an expected sub-exponential rate of convergence to the nonhyperbolic origin.

For this bifurcation we note that there can be a transfer of stability from the original cycle to the stability of the new cycle; we have already mentioned that at bifurcation the equilibrium P_0 is nonhyperbolic and has eigenvalue $d_0 = \gamma_0 = 0$; nonetheless λ may be computed from (5). This coincides with the stability quotient for the Guckenheimer-Holmes cycle. The cycle is stable if $\rho > 1$ where

$$\rho = \frac{c_0 c_1 c_2}{e_0 e_1 e_2}$$

assuming the new equilibrium on the z-axis is close to the origin. Figure 7 shows λ and ρ plotted against γ_0 for (4) except for $\gamma_1 = -0.6$ and $\gamma_3 = -0.1$; observe the continuous (but not differentiable) change of the stability quotient from one cycle to the other, passing through $\gamma_0 = 0$. Figure 8 shows this more clearly, while also showing a number of bifurcations in the system.

3.2 Case 1b: Local bifurcations at P_1

We now examine bifurcations of P_1 leading to destruction of the cycle. Bifurcation in the x direction will occur generically as a saddle node and this can result for example in bifurcation to an attracting equilibrium further out on the x-axis with hysteresis. The other bifurcations are of more interest and will be pitchfork bifurcations generically.

3.2.1 Bifurcation of P_1 in y-direction; stabilization of P_1

If P_1 bifurcates in the y direction, this bifurction must be supercritical and bifurcation will lead to stabilization of P_1. This bifurcation can go straight to an attracting heteroclinic cycle as $e_1 \to 0$ means that $\lambda \to \infty$.

3.2.2 Bifurcation of P_1 in z-direction; essential asymptotic stability

A bifurcation of P_1 in the z direction is a transverse bifurcation of the cycle [Chossat *et al.*, 1997] that leads to P_1 having a two dimensional unstable manifold. Nonetheless the stability cal-

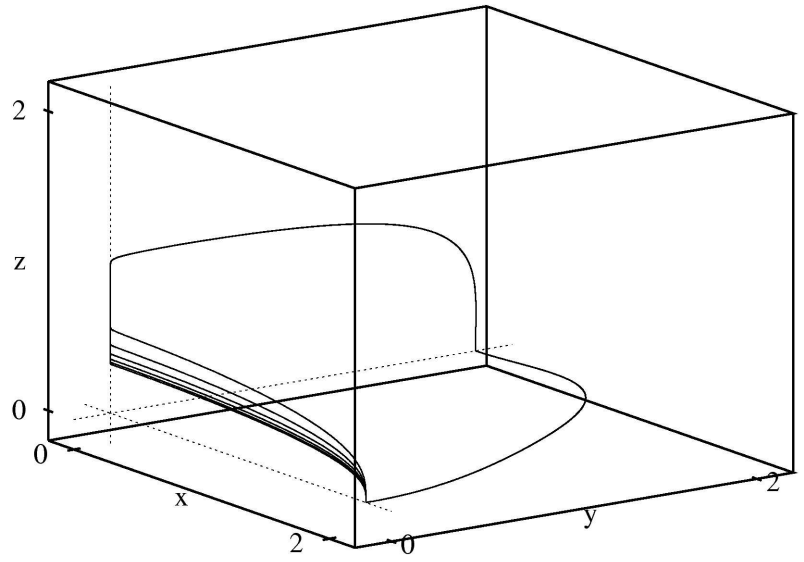

(a)

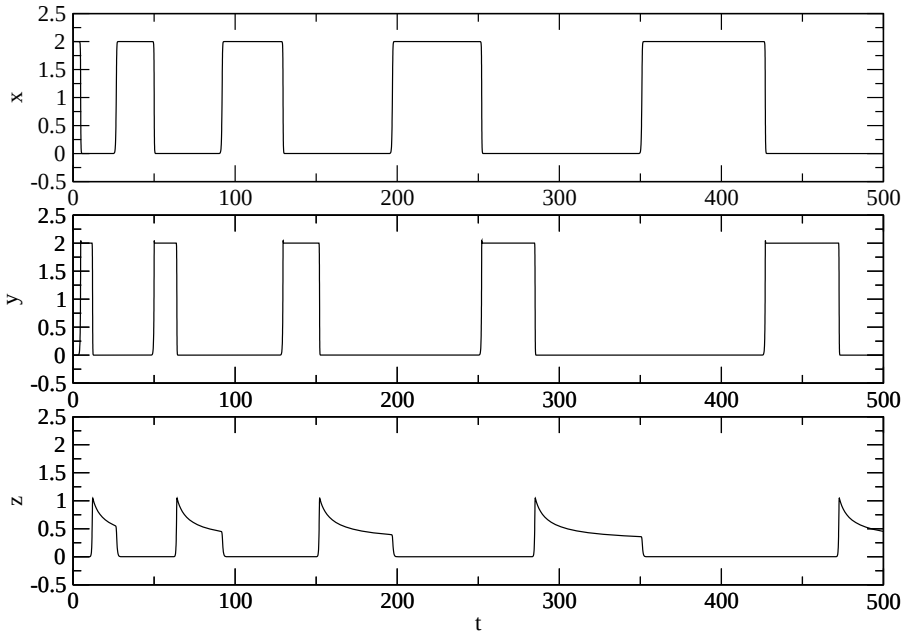

(b)

Figure 6: (a) shows a cycle of Guckenheimer-Holmes type bifurcated from the cycle shown in Figure 1, where the parameter values are as in equation (4) except for $\gamma_3 = -0.1$, $\gamma_1 = -0.6$ and $\gamma_0 = 0.01$. Meanwhile (b) shows the time series plot for the same parameters but with $\gamma_0 = 0$ where we are at the bifurcation point to this cycle.

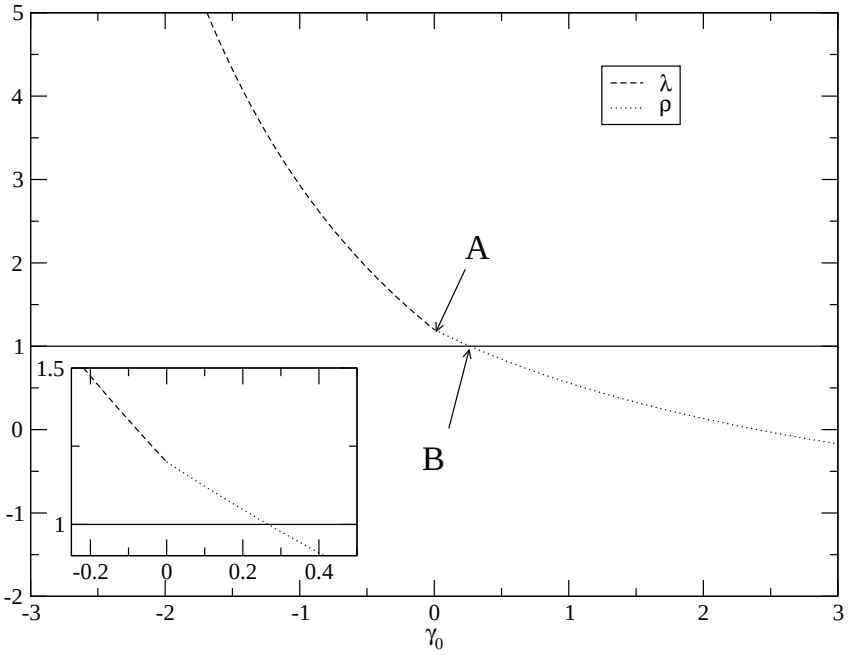

Figure 7: The values of the stability quotients λ and ρ on changing the parameter γ_0 where additionally $\gamma_1 = -0.6$ and $\gamma_3 = -0.1$. This allows us to observe a bifurcation to the Guckenheimer-Holmes cycle in Figure 6 for $\gamma_0 > 0$.

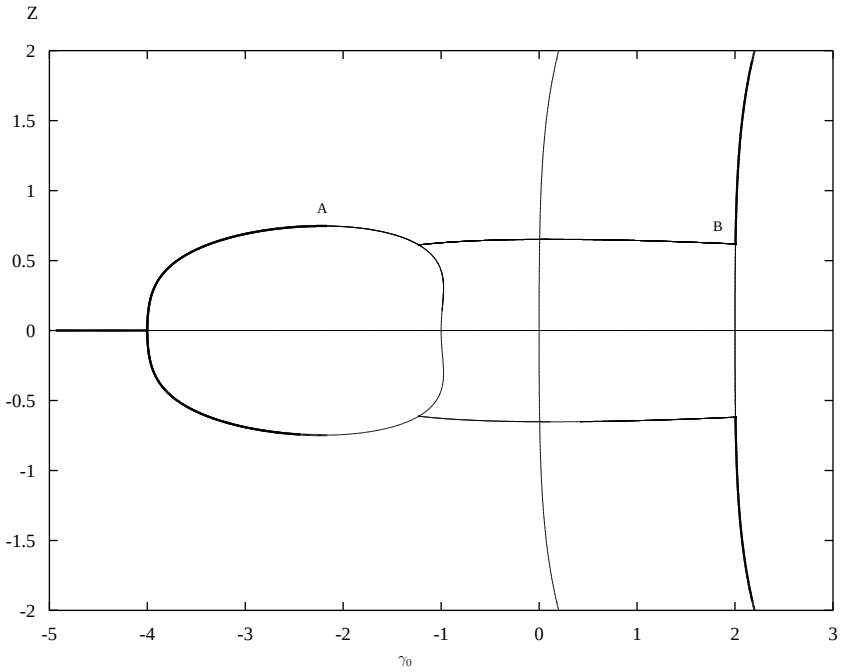

Figure 8: Bifurcation diagrams produced in AUTO showing branches of equilibria for (4) on varying γ_0, showing the z values of the branches. Robust heteroclinic cycles are found in the region enclosed by the points A and B; negative values of γ_0 give our original cycle, and the Guckenheimer-Holmes style cycle appears for positive values up to B at $\gamma_0 = 2$ where the only attractor becomes a sink at $(2, 0, z)$. In practice we see a limit cycle in (y,z) when approaching A from about $\gamma_0 < -2.06$. Note that a bifurcation of case 3 occurs as in Figure 13 upon decreasing γ_0 below the point A at $\gamma_0 = -2.16$. Note that the resonance at $\gamma_0 = 0$ cooincides with the bifurcation point.

culation in Section 2.1 is still valid and predicts that the original cycle can still be stable (see below), even though in this case c_1 is negative.

As an example, consider (3,4) changing the parameters $\beta_0 = -5$, $\gamma_0 = -1.5$ $\gamma_3 = 0.5$ and varying γ_1. When it is increased through 0.375, the eigenvalue c_1 passes through zero. However, the cycle still retains some stability: in the terminology of Melbourne [1991] the change in sign of c_1 causes the cycle to go from being asymptotically stable to being *essentially asymptotically stable*. This means that, local to the connection from P_0 to P_1, the basin of the cycle is still open but does not have full measure in some neighbourhoods of the connection.

3.3 Case 1c: Local bifurcations at P_2

A bifurcation of P_2 in the x direction cause a resonance bifurcation before the eigenvalue becomes zero (note that $c_2 = 0$ means that $\lambda = 0$) and hence this will not occur as a generic instability from the robust attracting cycle.

3.3.1 Bifurcation of P_2 in y-direction; limit cycle in (x, y) plane

The only generic bifurcation of P_2 in the y-direction will be a saddle-node bifurcation with another equilibrium in the y axis. If there are no other equilibria in this axis, this can lead to bifurcation to a limit cycle of large period in the (x, y)-plane as we now demonstrate.

For example, consider (3,4) and vary β_0 to give bifurcation as P_2 and Q_0 meet in the y-axis. At $\beta_0 = -6.25$, the heteroclinic cycle disappears and is replaced by a limit cycle contained wholly in the (x, y) plane. (Note also that the point Q_1 has also vanished; this bifurcates at $\beta_0 \approx -4.07$ but there are additional points Q_2 are now present in the (x, y) plane which appear at $\beta_0 \approx -5.38$). All these bifurcations can be observed in the diagram in Figure 11.

Figure 9 shows the limit cycle at a point just after the bifurcation at $\gamma_0 = -6.25$. Meanwhile Figure 10 schematically shows the saddle-node bifurcation local to P_2; for (a) and (b) there is a cycle with a connection entering in the (x, y) plane and leaving along the unstable manifold of P_2. For (c) the connection is broken and the simplest consistent dynamics will give that the unstable manifold of P_1 converges to a limit cycle in the x, y plane.

3.3.2 Bifurcation of P_2 in the z-direction; stabilization of P_2

The final local bifurcation we discuss is when e_2 goes to zero; this is generically a pitchfork bifurcation and must be subcritical to give bifurcation directly from the cycle. Such a bifurcation will lead to the stable cycle being replaced by a stable equilibrium at P_2. In Figure 8 this can be observed for (3,4) when γ_0 passes below -4.

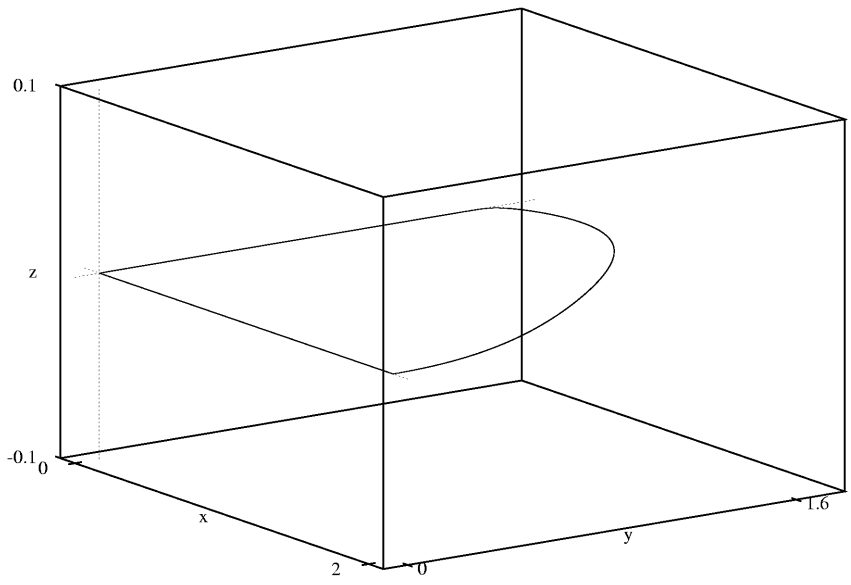

Figure 9: The limit cycle produced in the (x, y) plane after bifurcation from the cycle in Figure 1 caused by a saddle-node bifurcation of the equilibria P_2 and Q_0. In this example $\beta_0 = -6.3$.

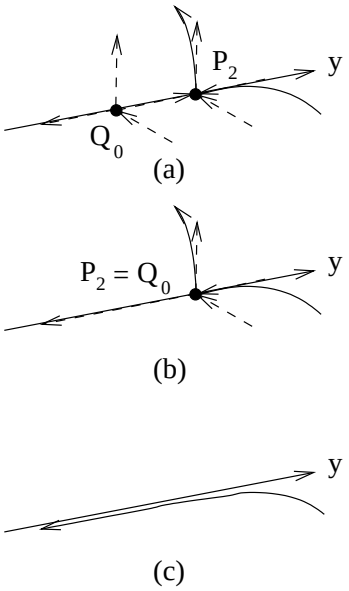

Figure 10: Schematic diagram showing the bifurcation to a limit cycle in the (x, y) plane caused by a saddle-node bifurcation of P_2 and Q_0. This can occur with a stable heteroclinic cycle between the P_i in (a) being replaced by a global limit cycle, a part of which is shown in (c).

3.4 Case 2: Bifurcations of the connecting orbits

Another possible type of generic (codimension one) bifurcation in which the cycle can lose stability is a bifurcation that destroys a connecting orbit. We have there are two generic bifurcations that lead to destruction of the cycle; either

(a) there is a saddle-node bifurcation on a connection that destroys the connection, or

(b) the connection becomes heteroclinic to another equilibrium not involved in the cycle.

These two possibilities are shown schematically in Figure 12 on varying a bifurcation parameter α through a bifurcation point at 0. In principle either of these bifurcations can occur on any of the connections.

Figure 13 shows an observed bifurcation of the connection between P_2 and P_0 of type (b) above on setting (4) and $\gamma_0 = -2.064318$. For γ_0 more negative than approximately this value the unstable manifold of P_2 approaches a limit cycle in the (y, z) plane surrounding Q_1 the spiral source in the (y, z) plane; for γ_0 more positive it forms a connection (shown by the dashed line) that means the cycle is present. At the bifurcation point there is a structurally unstable connection from P_2 to Q_0. A similar phase portrait can be obtained varying only β_0, though only by passing through a more complex limit cycle, as explained in Figure 11.

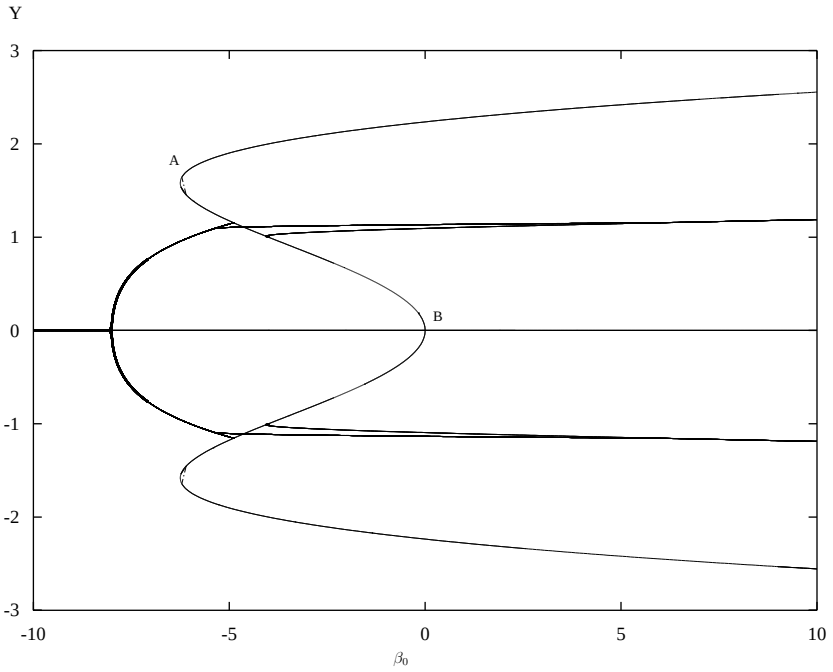

Figure 11: Bifurcation diagram showing branches of equilibria for (4) on varying β_0, showing y values of the branches. Note that bold lines indicate branches of stable equilibria, and thin lines those of unstable equilibria. There is a robust cycle of the form in Figure 1 for $-6.25 < \beta_0 \lesssim 0$. At the lower boundary (labelled A in the diagram) we have a bifurcation to a limit cycle in the (x, y) plane as outlined in 3.3.1. The upper boundary B corresponds to a resonance bifurcation at $\beta_0 = 0$. For β_0 positive there is a limit cycle close to the cycle.

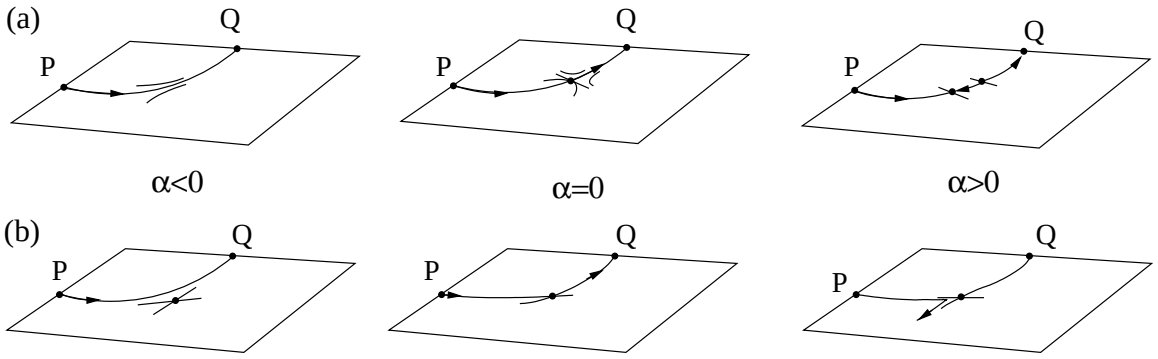

Figure 12: Schematic diagram showing two possible generic bifurcations that destroy a robust connecting orbit between hyperbolic equilibria P and Q on varying an arbitrary parameter α. In case (a) there is a saddle node at $\alpha = 0$; in case (b) the connecting orbit becomes heteroclinic to another saddle at $\alpha = 0$. In both cases the connection from P to Q is destroyed for $\alpha > 0$.

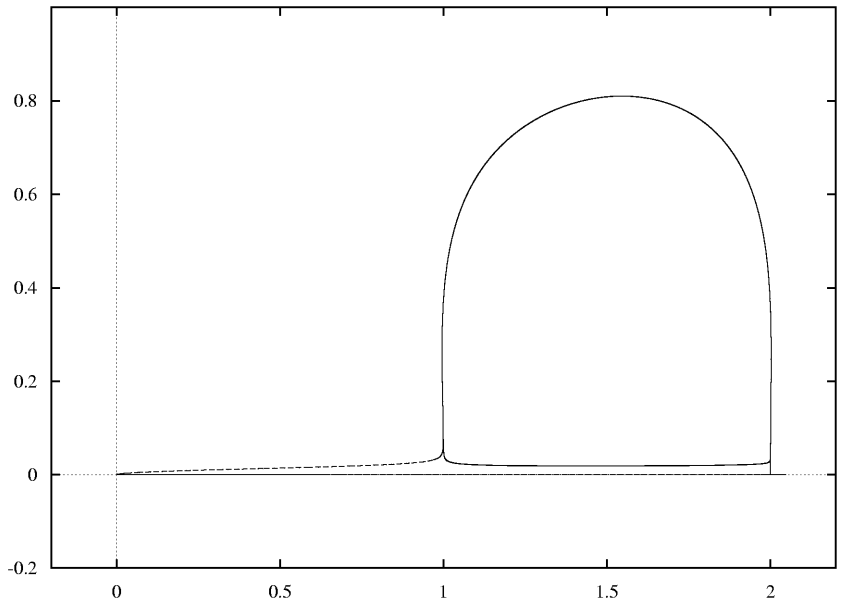

Figure 13: A bifurcation from a stable cycle of the type in Figure 1 to an attractor in the (y, z) plane, induced by the destruction of the connection between P_2 and P_0. The connection in the (y, z) plane is shown with $\gamma_0 = -2.064318$ approximately, varying in the 9th decimal place to show the two types of behaviour. The dashed line shows the heteroclinic connection, while the solid line shows the trajectory when γ_0 is decreased slightly.

3.5 Case 3: Resonance bifurcations of the cycle

As discussed in Section 2.1 the heteroclinic cycle Figure 1 can lose attraction at a resonance bifurcation at $\lambda = 1$ in (7). This can give rise to a branch of periodic solutions that bifurcate at resonance either sub- or super-critically. For instance, one can observe bifurcation to the limit cycle shown in Figure 14 with parameters as in (4) except for $\alpha_0 = 6.6$. In this case the stability coefficient is $\lambda = 0.62846 < 1$ indicating instability of the cycle.

More generally, one can verify that on varying only α_0 we have

$$\lambda = \frac{(12 - \alpha_0)4x_e^2}{3\alpha_0(2x_e^2 - 4)} \tag{10}$$

where $x_e^2 = \alpha_0$ and so there is a unique α_0 giving resonance $\lambda = 1$.

4 Discussion

In summary we have demonstrated the existence of an open set of smooth vector fields on $\mathbb{R}^3$ under the action of $G = (\mathbb{Z}_2)^3$ possessing attracting robust attracting heteroclinic cycles including the origin and we have classified the possible instabilities of these cycles. The polynomial example (3) shows this cycle for an open set of parameter values and allows analysis of examples of the possible bifurcations. Note that the example is a fifth order polynomial vector field, and such phenomena cannot be seen in a lower order polynomial simply through consideration of the number of equilibria needed. Although this system shows these cycles for an open set of parameter values, our experiments using random choice of parameters has shown that such cycles are very difficult to find.

Our examination of generic codimension one bifurcations has found cases of direct bifucation to attractors that are topologically equivalent other well-known examples of robust heteroclinic cycles in $\mathbb{R}^3$, namely the cycle of Guckenheimer and Holmes and a cycle that appears in $\mathbf{O}(2)$ mode interaction. We have also found direct bifurcation from an attracting heteroclinic cycle to stability of each of the equilibria in the cycle and to attracting limit cycles that follow closely connections in the cycle.

Of particular interest is the scenario where a subcritical pitchfork bifurcation of the origin in the x-direction gives rise to a robust heteroclinic to the origin as being the only attractor after bifurcation. This can be interpreted as a primary instability of a solution with maximal symmetry bifurcating to an attractor that it intermittent to the origin. It would be of great interest to find a physical system in which such a generic scenario can be identified.

These cycles can also appear in system of predator-prey type using a well-known equivalence (see e.g. [Krupa, 1997]). We set $X = x^2$, $Y = y^2$ and $Z = y^2$ and if we consider a flow that preserves extinction of any of these species, this will lead us to considering ODEs of the form (11)

$$\begin{aligned} \dot{X} &= X f_1(X, Y, Z) \\ \dot{Y} &= X f_2(X, Y, Z) \\ \dot{Z} &= X f_3(X, Y, Z) \end{aligned} \tag{11}$$

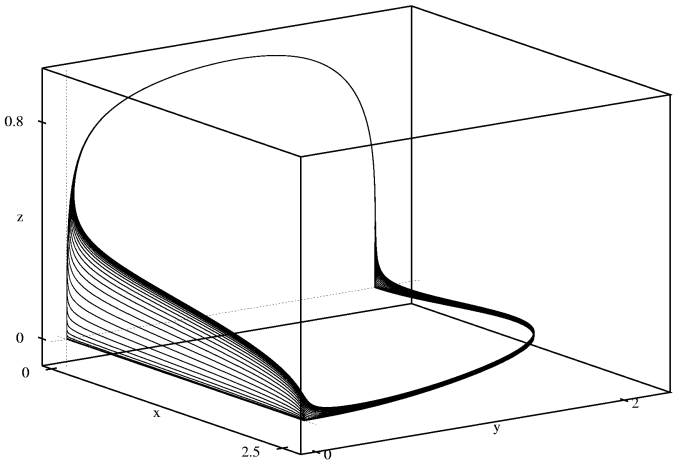

(a)

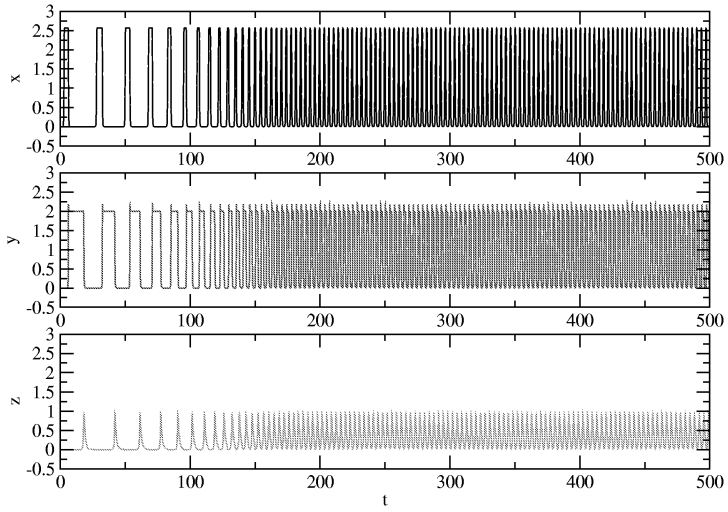

(b)

Figure 14: A trajectory attracted to the limit cycle bifurcating from the heteroclinic cycle in Figure 1 at a resonance at $\alpha_0 = 6$; here we have $\alpha_0 = 6.6$. We start close to the original heteroclinic cycle and converge to a limit cycle which continues to shadow the heteroclinic cycle. (a) shows the cycle in (x, y, z) space and (b) shows the timeseries of the trajectory shown in (a).

which can be seen to be equivalent to (2); in particular the robust cycle to the origin from Theorem 1 can also appear for an open set of such systems. This will occur for certain situations when X acts as a prey, Z a predator and Y a species that may switch its strategy depending on population size. The presence of the attracting cycle predicts the eventual extinction of two or three of the species depending on which species first goes under the threshold of one organism.

4.1 Other situations giving robust cycles to the origin

The dynamics we have discussed provides a model to understand bursting maximal symmetry states; which has been observed previously for example by Moehlis and Knobloch [2000] in systems with broken $\mathbf{D}_4$ symmetry. In their models the bursting occurs only in the presence of symmetry breaking terms; our model does not need this. However, in the presence of low noise or symmetry breaking, a neighbourhood of our heteroclinic cycle will still remain attracting and so the intermittency will be observable.

We believe that this is in some sense the simplest symmetry and phase space in which a robust attracting heteroclinic to the origin can appear. The group $G = \mathbb{Z}_2$ is not sufficient as is any group acting orthogonally on $\mathbb{R}^2$; to obtain a robust cycle one needs at least two invariant subspaces with dimension strictly greater than zero and strictly less than that of phase space. For $G = (\mathbb{Z}_2)^2$ on $\mathbb{R}^3$ one can obtain robust heteroclinic cycles (see for example Figure 4). However, this gives two equilibria of maximal symmetry included in the cycle and so manifest itself as a robust cycle to distinct maximal symmetry solutions. Hence it is difficult to imagine a group with lower order giving such cycles.

We strongly suspect that similar robust cycles will be found for example systems with $\mathbf{O}(2)$ symmetry; several authors have noted stable heteroclinic cycles in these systems for $\mathbb{R}^4$, see for example Porter and Knobloch [2001] and Armbruster *et al.* [1988]. Bifurcations from an $\mathbf{O}(2)$ and the Guckenheimer-Holmes cycles have also been examined by Sandstede and Scheel [1995].

Acknowledgements

PA would like to thank Ian Melbourne, Rob Sturman and Alastair Rucklidge for stimulating conversations regarding these cycles. DH would like to acknowledge support of the EPSRC.

References

[Armbruster *et al.*, 1988] D Armbruster, J Guckenheimer and P Holmes [1988] "Heteroclinic cycles and modulated travelling waves in systems with $\mathbf{O}(2)$ symmetry", *Physica D* **29**, 257–282.

[Ashwin & Field, 1999] P Ashwin and M J Field [1999] "Heteroclinic networks in coupled cell systems", *Arch. Rat. Mech. & Anal.* **148**, 107–143.

[Ashwin & Montaldi, 2002] P Ashwin and James Montaldi [2002] "Group theoretic conditions for existence of robust relative homoclinic trajectories", *Math. Proc. Camb. Phil. Soc.* **133**, 125-141.

[Chossat *et al.*, 1997] P Chossat, M Krupa, I Melbourne and A Scheel [1997] "Transverse bifurcations of homoclinic cycles", *Physica D* **100**, 85–100.

[Chow *et al.*, 1990] S-N Chow, B Deng and B Fiedler [1990] "Homoclinic bifurcation at resonant eigenvalues", *J. Dynam. Differential Equations* **2**, 177–244.

[Field, 1996] M Field [1996] "Lectures on Dynamics, Bifurcation and symmetry", *Pitman Research Notes in Mathematics*, **356**, Pitman.

[Field & Swift, 1991] M Field and J Swift [1991] "Stationary bifurcation to limit cycles and heteroclinic cycles", *Nonlinearity* **4**, 1001–1043.

[Golubitsky *et al.*, 1988] M Golubitsky, IN Stewart and DG Schaeffer [1988] "Groups and Singularities in Bifurcation Theory, Vol. 2", *Appl. Math. Sci. 69, Springer.*

[Guckenheimer & Holmes, 1988] J Guckenheimer and P Holmes [1988] "Structurally stable heteroclinic cycles", *Math. Proc. Camb. Phil. Soc.* **103**, 189–192.

[Kevrekidis *et al.*, 1990] IG Kevrekidis, B Nicolaenko and JC Scovel [1990] "Back in the saddle again: a computer assisted study of the Kuramoto Sivashinsky equation", *SIAM J. Appl. Math* **50**, 760–790.

[Kirk & Silber, 1994] V Kirk and M Silber [1994] "A competition between heteroclinic cycles", *Nonlinearity* **7**(6), 1605–1621.

[Krupa, 1997] M Krupa [1997] "Robust heteroclinic cycles", *Journal of Nonlinear Science* **7**, 129–176.

[Krupa & Melbourne, 1995] M Krupa, I Melbourne [1995] "Asymptotic stability of heteroclinic cycles in systems with symmetry", *Ergodic Theory and Dyn. Sys.* **15**, 121–147.

[Krupa & Melbourne, 2004] M Krupa, I Melbourne [2004] "Asymptotic stability of heteroclinic cycles in systems with symmetry, II", To appear in *Proc. Roy. Soc. Edinburgh A*.

[Melbourne, 1991] I Melbourne [1991] "An example of a non-asymptotically stable attractor", *Nonlinearity* **4**, 835–844.

[Melbourne *et al.*, 1989] I Melbourne, P Chossat and M Golubitsky [1989] "Heteroclinic cycles involving periodic solutions in mode interactions with $\mathbf{O}(2)$ symmetry", *Proc. Roy. Soc. Edinburgh* **113A**, 315–345.

[Moehlis & Knobloch, 2000] J Moehlis and E Knobloch [2000] "Bursts in oscillatory systems with broken D_4 symmetry", *Physica D* **135**, 263–304.

[Perko, 2001] L Perko [2001] *Differential Equations and Dynamical Systems (Third Edition)* (Springer).

[Porter & Knobloch, 2001] J Porter and E Knobloch [2001] "New type of complex dynamics in the 1:2 spatial resonance", *Physica D* **159**, 125–154.

[Sandstede & Scheel, 1995] B Sandstede and A Scheel [1995] "Forced symmetry breaking of homoclinic cycles", *Nonlinearity* **8**, 333–365.

A Calculation of the heteroclinic cycle stability

In this appendix we detail the derivation of the approximate return map (7). We choose linearising coordinates within neighbourhoods of the P_i for and express our return map in terms of these. We parametrize the surfaces of section shown in Figure 2 by

$$\begin{array}{ll} \Pi_0^{\text{in}} = (x, y, \epsilon) & \Pi_0^{\text{out}} = (\epsilon, y, z) \\ \Pi_1^{\text{in}} = (\epsilon, y, z) & \Pi_1^{\text{out}} = (x, \epsilon, z) \\ \Pi_2^{\text{in}} = (\epsilon, y, z) & \Pi_2^{\text{out}} = (x, y, \epsilon) \end{array}$$

and note that the F_i are given by the flows of the ODEs

$$F_0 \quad \begin{cases} \dot{x} = e_0 x \\ \dot{y} = -c_0 y \\ \dot{z} = -d_0 z \end{cases}$$

$$F_1 \quad \begin{cases} \dot{x} = -d_1 x \\ \dot{y} = e_1 y \\ \dot{z} = -c_1 z \end{cases}$$

$$F_2 \quad \begin{cases} \dot{x} = -c_2 x \\ \dot{y} = -d_2 y \\ \dot{z} = e_2 z. \end{cases}$$

Solving these we obtain

$$F_0(x, y, \epsilon) = (\epsilon, y x^{\frac{c_0}{e_0}} \epsilon^{\frac{-c_0}{e_0}}, \epsilon x^{\frac{d_0}{e_0}} \epsilon^{\frac{-d_0}{e_0}}),$$

also

$$F_1(\epsilon, y, z) = (\epsilon^{1-\frac{d_1}{e_1}} y^{\frac{d_1}{e_1}}, \epsilon, z \epsilon^{\frac{-c_1}{e_1}} y^{\frac{c_1}{e_1}}),$$

and

$$F_2(\epsilon, y, z) = (\epsilon^{1-\frac{c_2}{e_2}} y^{\frac{c_2}{e_2}}, y \epsilon^{\frac{-d_2}{e_2}} z^{\frac{d_2}{e_2}}, \epsilon).$$

The connecting maps G_i have generic non-degenerate linear parts that respect the action of the group $G = (\mathbb{Z}_2)^3$ and so the linearized maps are

$$\begin{array}{l} G_0(\epsilon, y, z) = (\epsilon, a_0 y, a_1 z), \\ G_1(x, \epsilon, z) = (\epsilon, a_2 + a_3 x + a_4 z, a_5 z), \\ G_2(x, y, \epsilon) = (a_6 x, a_7 + a_8 x + a_9 y, \epsilon) \end{array}$$

where the a_i are all real numbers that may be assumed to be non-zero. Putting these together and starting at (x, y, ϵ) we get

$$G_0 \circ F_0 = (\epsilon, a_0 y x^{\frac{c_0}{e_0}} \epsilon^{\frac{-c_0}{e_0}}, a_1 x^{\frac{d_0}{e_0}} \epsilon^{1-\frac{d_0}{e_0}})$$

and then

$$F_1 \circ G_0 \circ F_0 = (Ax^{\frac{d_1 c_0}{e_1 e_0}} y^{\frac{d_1}{e_1}}, \epsilon, Bx^{\frac{d_0 e_1 + c_1 c_0}{e_1 e_0}} y^{\frac{c_1}{e_1}}),$$

$$G_1 \circ F_1 \circ G_0 \circ F_0 = (\epsilon, C + Dx^{\frac{d_1 c_0}{e_1 e_0}} y^{\frac{d_1}{e_1}} + Ex^{\frac{d_0 e_1 + c_1 c_0}{e_1 e_0}} y^{\frac{c_1}{e_1}}, Fx^{\frac{d_0 e_1 + c_1 c_0}{e_1 e_0}} y^{\frac{c_1}{e_1}}),$$

then

$$\begin{aligned} F_2 \circ G_1 \circ F_1 \circ G_0 \circ F_0 = \quad & (Gx^{\frac{c_2(d_0 e_1 + c_1 c_0)}{e_2 e_1 e_0}} y^{\frac{c_2 c_1}{e_2 e_1}}, \\ & Hx^{\frac{d_2(d_0 e_1 + c_1 c_0)}{e_2 e_1 e_0}} y^{\frac{c_1 d_2}{e_1 e_2}} \\ & + Ix^{\frac{d_2(d_0 e_1 + c_1 c_0) + e_2 d_1 c_0}{e_2 e_1 e_0}} y^{\frac{c_1 d_2 + d_1 e_2}{e_1 e_2}} \\ & + Jx^{\frac{d_2(d_0 e_1 + c_1 c_0) + e_2(d_0 e_1 + c_1 c_0)}{e_2 e_1 e_0}} y^{\frac{c_1 d_2 + c_1 e_2}{e_1 e_2}}, \epsilon) \end{aligned}$$

and finally

$$\begin{aligned} F = G_2 \circ F_2 \circ G_1 \circ F_1 \circ G_0 \circ F_0 = \quad & (Kx^{\frac{c_2(d_0 e_1 + c_1 c_0)}{e_2 e_1 e_0}} y^{\frac{c_2 c_1}{e_2 e_1}}, \\ & L + Mx^{\frac{d_2(d_0 e_1 + c_1 c_0)}{e_2 e_1 e_0}} y^{\frac{c_1 d_2}{e_1 e_2}} \\ & + Nx^{\frac{d_2(d_0 e_1 + c_1 c_0) + e_2 d_1 c_0}{e_2 e_1 e_0}} y^{\frac{c_1 d_2 + d_1 e_2}{e_1 e_2}} \\ & + Px^{\frac{d_2(d_0 e_1 + c_1 c_0) + e_2(d_0 e_1 + c_1 c_0)}{e_2 e_1 e_0}} y^{\frac{c_1 d_2 + c_1 e_2}{e_1 e_2}}, \epsilon) \end{aligned} \tag{12}$$

where at each stage the parameters A, B etc only depend on ϵ, the a_i and the eigenvalues c_i, d_i and e_i. One can then identify the leading order terms in (12) depending on the signs of the eigenvalues.